REGULAR ARTICLE

Incorporation of Thiadiazole Derivatives as π -Spacer to Construct Efficient Metal-free Organic Dye Sensitizers for Dye-sensitized Solar Cells: A Theoretical Study

Wenjie Fan and Wei-qiao Deng*

*State Key Laboratory of Molecular Reaction Dynamics, Dalian National Laboratory for Clean Energy, Dalian Institute of Chemical Physics, Chinese Academy of Sciences; Dalian, Liaoning 116023, P. R. China Received 18 January 2013; Accepted (in revised version) 25 February 2013

Special Issue: Guo-Zhong He Festschrift

Abstract: Based on theoretical calculations, we studied four triphenylamine (TPA)-based dyes (namely D1-D4) incorporating electron-deficient thiadiazole derivatives as the π -spacer for the applications in dye-sensitized solar cells (DSSCs). The effects of the electron-deficient units on the spectra and electrochemical properties have been investigated by the combination of density functional tight-binding (DFTB), density functional theory (DFT), and time-dependent DFT (TDDFT) approaches. Compared with the model compound D0, which adopts a phenylene unit as the π -spacer, D1-D4 dyes display remarkably enhanced spectral responses in the red portion of the solar spectrum and possess desirable energetic properties once anchored on TiO₂ surface. The newly constructed dyes D2, D3, and D4 demonstrate desirable energetic and spectroscopic parameters, and may lead to efficient metal-free organic dye sensitizers for DSSCs.

AMS subject classifications: 65D18, 68U05

Key words: DSSCs; triphenylamine dyes; DFT calculations

^{*} Corresponding author. *Email address*: <u>dengwq@dicp.ac.cn</u> (W.-Q. Deng)

1 Introduction

Dye sensitized solar cells (DSSCs) are currently receiving significant attention as a low-cost and high-efficiency alternative to inorganic semiconductor-based photovoltaic devices for the conversion of sunlight into electricity [1-4]. The DSSCs are made of three parts: (i) a wide band gap semiconductor (usually TiO₂) deposited on a translucid conducting substrate; (ii) an anchored molecular sensitizer; and (iii) a redox electrolyte (usually I⁻/I₃-). Photosensitizers have been investigated to play a significant role for efficient DSSCs. Ruthenium photosensitizers have shown very impressive solar-to-electric power conversion efficiencies exceeding 11% under standard illumination [5, 6]. Taking account of the limited Ru resource and the environmental issues, metal-free organic dyes have attracted increasing interest as the substitute for the Ru complexes in recent years, owing to their crucial advantages including the flexibility in tailoring their molecular structures, high molar extinction coefficients, and low cost [7]. Recently, novel organic dyes based coumarin, perylene, triphenylamine (TPA), indoline, squaraine, and other organic units have been studied for applications in DSSCs [8-12]. Especially, TPA-based organic dyes, with TPA derivatives and the cyanoactetic acid moiety as electron donor and electron acceptor units, respectively, have displayed prominent light-to-electrical energy conversion efficiencies reaching 10% in DSSCs [12]. The TPA group with a sizable steric hindrance is expected to greatly confine the cationic charge from the TiO₂ surface and prevent unfavorable dye aggregation at the TiO₂ surface. The structural modifications of TPA-based organic dyes have been investigated intensively [7,13-16]. Most of the efficient organic sensitizers are made of the donor- $(\pi$ -spacer)-acceptor (D- π -A) system. Using sensitizers with high molar extinction coefficients that extend throughout the visible and into the near-IR regions is desirable for efficient solar to energy conversion. Organic sensitizers with long π -conjugations had been demonstrated to augment the molar extinction coefficients and enhance panchromatic light harvesting, thus giving desirable DSSC efficiency and stability [12,15,17,18].

For organic sensitizers, one of the main drawbacks remains the sharp and narrow absorption bands in the visible region, which impairs the light-harvesting capabilities. One effective method to lower the highest occupied molecular orbital (HOMO)-the lowest unoccupied molecular orbital (LUMO) gap is by lifting the energy of HOMO while at the same time maintain the suitable LUMO energy level. For example, Wang group has reported that adding one electron-rich 3,4-ethylenedioxythiophene unit in organic dye C217 results in a evident 0.18 eV lift of the HOMO, compared to dye C206, thus narrowing the HOMO and LUMO gap and enhancing the extinction coefficients [12]. Another effective method to lower the HOMO-LUMO gap is by lowering the LUMO orbitals and meanwhile maintains the low

HOMO energy level for efficient dye degenerations. Recently, the electron-withdrawing terephthalonitrile [16] or electron-deficient heteroarenes [19-25] including pyrimidine [22] and benzothiadiazole [23-25] unites have been incorporated to the cyanoacrylic acid of the $D-\pi-A$ dyes to lower the LUMO energy levels. The newly designed dyes showed more red-shifted absorption band and enhanced the light harvesting than their electron-rich analogues, such as thiophene derivatives [26], furan [27], and pyrrole [28]. Lin and coworkers have reported a series of organic sensitizers with diphenylthienylamines donors and cyanoacrylic acid acceptors bridged by an electron-deficient pyrimidine unit, and they found that the new dyes demonstrate bathochromic shift in absorption and effectively improve the light harvesting and the overall conversion efficiency, due to the advantage of the characteristic planarity and electronic deficiency of pyrimidine [22]. Lee et al. have reported a series of π -conjugated TPA organic dyes with the incorporation of the benzothiadiazole moieties as the electron acceptor/anchoring groups, and the new dyes are shown to red-shift the absorption band in UV/Visible spectrum due to the longer π conjugation and narrower HOMO-LUMO gap [23]. Justin Thomas and coworkers demonstrated that the introduction of electron-deficient dithienylbenzothiadiazole moiety to the anthracene-based TPA dye results in a 50nm red-shifted band and an increase in intensity on elongation of the conjugation. Their works clearly demonstrate that benzothiadiazole remarkably alters the dye's electronic structure and reduces the HOMO-LUMO gap by lowering the LUMO level [24, 25].

The overall conversion efficiency (η) of the DSSCs is determined by four parameters: the short current density (Jsc), the open circuit potential (Voc), the fill factor (ff) of the cell, and the intensity of the incident light (Is), as shown in equation (1):

$$\eta = J_{SC}V_{OC}ff/I_{s} \tag{1}$$

Jsc is related to the rate of electron injection to the semiconductor conduction band, and Voc is determined by the energy difference between the semiconductor conduction band edge and the mediator redox potential. According to eqn (1), in order to improve η , the product of Voc and Jsc should be optimized. A smaller HOMO-LUMO gap is needed to achieve a higher Jsc, while the low HOMO energy level should still be maintained for efficient dye regeneration. You and coworkers have reported that the LUMO of donor–acceptor copolymers largely locates on the acceptor moiety, and the bandgap can be reduced by incorporating a electron deficient unit to lower the LUMO while at the same time maintain the HOMO energy level [29-32].

Inspired by recent experimental progress on the TPA organic dyes and You group's

research mentioned above, here we constructed a series of organic D- π -A dyes, in which TPA donors and cyanoacrylic acid acceptors are bridged by various electron-deficient thiadiazole derivatives. The electron-deficient units considered 2,1,3-benzothiadiazole (BT) and thiadiazolo[3,4-c]pyridine (PyT), which have been shown to lower the LUMO levels of the organic molecules while at the same time maintain the HOMO levels, thus leading to a smaller HOMO-LUMO gap, and a more red-shifted UV/Vis [23-25,27-30]. To further lower the **HOMO-LUMO** spectrum naphtho[2,1-b:3,4-b']dithiophene (NDT) unit is connected to BT or PyT to lift the HOMO energy levels. The structures of the dyes studied in this work are shown in Figure 1, in which TPA moiety is used as electron-donating moiety, cyanoacrylic acid as electron acceptor, and electron-deficient units BT, PyT, NDT-BT, and NDT-PyT are involved as π -conjugations to bridge the donor-acceptor systems. The new TPA dyes are denoted as D1 to D4. A model dye D0 with phenylene as the π -spacer was also studied for parallel comparison. For D1 and D2, the only structural difference is that D1 contains a BT unit while D2 has a PyT unit. A distinguishable feature of D3 and D4 is the binary spacer involved, with a NDT unit connected to the donor part. Similar to the organic dyes HKK-BTZ1-4 reported recently [23], a thiophene ring is connected to the acceptor cyanoacrylic acid for better conjugation of the dye. The combination of density functional tight-binding (DFTB), density functional theory (DFT), and time-dependent DFT (TDDFT) approaches is employed to demonstrate the effects of the electron-deficient units on the spectra and electrochemical properties of the TPA organic dyes. To examine the electronic coupling between dye's LUMO and the TiO₂ conduction band, we also investigated the dye/(TiO₂)₄₆ interacting system.

Figure 1: Molecular structures of 5 metal-free TPA based organic dyes (D0-D4) bridged by different π linkers.

2 Computational Details

The optimizations of the ground state structures are performed by means of DFT or self-consistent-charge density-functional tight-binding (SCC-DFTB) theory [33]. The electronic structures and vertical electronic excitation energies are determined with DFT and TDDFT methods. For the ground-state geometric optimization of the pure dyes, B3LYP/6-31G(d,p) is selected, for the good performance of the geometry optimization for some TPA derivatives [34]. For the TDDFT calculations of the pure organic dyes considered in this work, 5 funcionals are considered, including one pure density functional PW91 [35], three hybrid B3LYP [36], PBE0 [37] and BHandH [38] functionals, including 20%, 25% and 50% of Hartree-Fock (HF) exchange, respectively, and CAM-B3LYP functional [39] which is the Handy and co-workers' long-range corrected version of B3LYP using the Coulomb-attenuating method. Solvation effects were investigated performing TDDFT calculations in various solvents with the nonequilibrium version of the C-PCM model [40] implemented in Gaussian09 program [41].

For the organic dye/(TiO₂)₄₆ interacting systems with more than 200 atoms, we take the advantages of the efficiency and reliability of the DFTB method for geometry optimizations. The full geometric optimizations were performed using the conjugate gradient algorithm until the residual forces were below 5×10⁻⁴ au, and the charge convergence criterion is 10⁻⁵ electrons. A comprehensive description of the DFTB method can be found in the literature [33,42]. The DFTB optimized dye/(TiO₂)₄₆ nanoparticle were followed by single point electronic structure analysis, for which we used the B3LYP functional together with a popular used 6-31G(d) basis set, as implemented in the Gaussian09 program package. The consistency of the results received with different codes is always kept under control.

3 Results and Discussion

3.1 Molecular orbital features

All the five dyes show structural similarities, with a TPA moiety as the electron-donor and hydrophilic cyanoacrylic acid electron-acceptor. The difference between the dyes is the linker part with different modifications. For the optimized structures, there is coplanarity between the anchoring group and the bridging unit, which is favorable for the electron transfer. **Figure 2** shows the frontier orbitals of the HOMO and the LUMO of the dyes. The HOMO of dyes is mainly populated over the TPA group and its adjacent thiophene/electron-deficient units, while the LUMO is delocalized through the cyanoacrylic

acid and its adjacent thiophene/electron deficient group, which is an ideal spatial orientation of molecular orbital conditions for DSSCs. **Figure 2** also confirms the highly delocalized character of the frontier orbitals, which is a typical feature of cyanine-like systems.

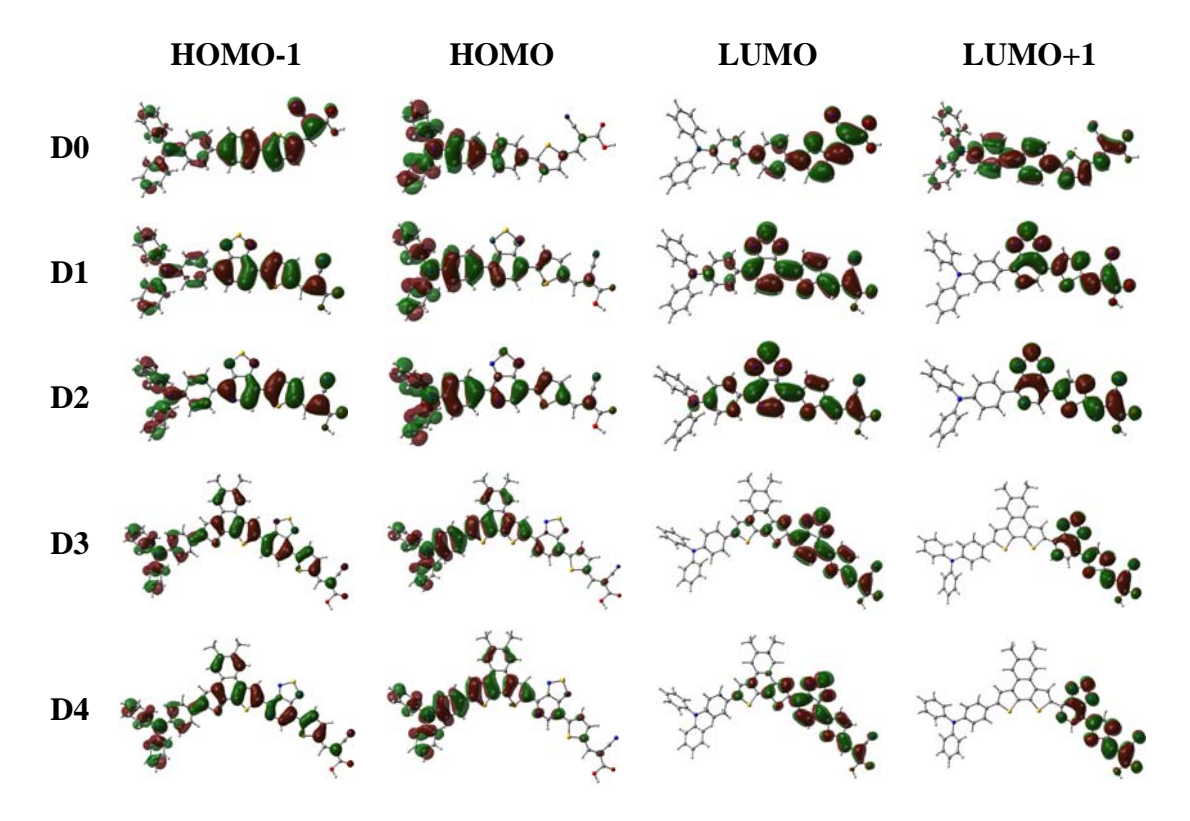


Figure 2: Isosurfaces of the selected frontier orbitals of the TPA dyes D0-D4 at B3LYP/6-31G(d,p) in gas phase. The isovalue is 0.02 au.

3.2 Energy levels

Suitable energy levels and the proper locations of HOMO and LUMO orbitals of the dye sensitizer are required to match the potential of iodine/iodide redox and the conduction band edge level of the TiO₂ [43]. The highest few occupied and lowest few unoccupied orbitals are particularly interesting, since they are involved in the electron transitions, in which the photoinduced electron transfers from the excited-state dye to the semiconductor surface. **Figure 3** depicts the HOMO-1, HOMO, LUMO, LUMO+1 energy levels of these TPA dyes at B3LYP/6-31G(d,p) level of theory. We found from **Figure 3** that the orbital levels of TPA dyes studied here are very sensitive to a change in the π -bridge unit. Incorporating the electron-deficient thiadiazole derivatives into the π bridge effectively lowers the LUMO energy level and thus narrows the band gap of the dyes.

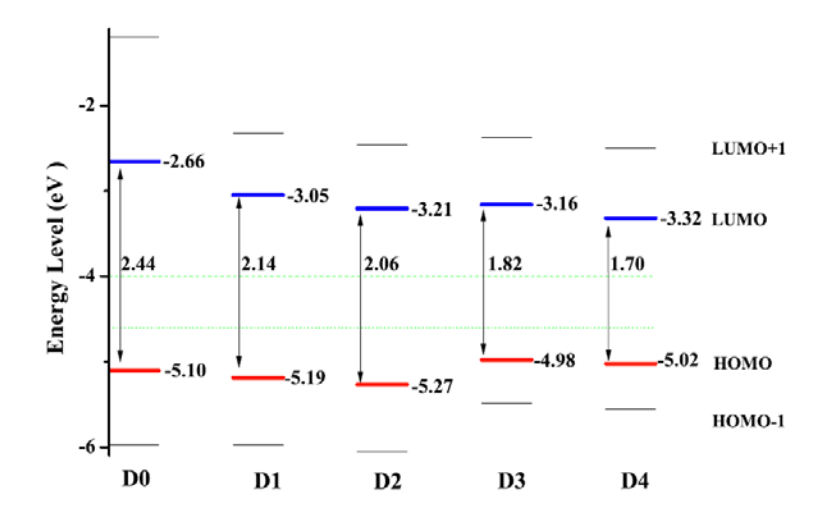


Figure 3: Computed energy levels and HOMO-LUMO gaps for the TPA dyes at B3LYP/6-31G(d,p) level of theory, together with the experimental TiO₂ CB edge (dash) and I⁻/I₃ redox level (dot).

The BT unit is a low-band gap chromophore, and it can alter the electronic structure of the sensitizer significantly and reduces the band gap remarkably by lowering the LUMO energy level, therefore leading to a red-shifted adsorption spectrum, and our theoretical results agree with previous work [24]. The inclusion of BT unit in the conjugation pathway shifts the LUMO toward the cyanoacrylic acid segment. Replacing benzene unit with the highly electron-deficient BT unit in D1 effectively lowers the LUMO of D1 to -3.05 eV via intramolecular charge transfer compared with that of D0 (-2.66 eV). Meanwhile the HOMO energy levels of D0 and D1 are basically similar. Due to the significant decrease of LUMO level, the HOMO-LUMO gap of D1 is 0.3 eV smaller than that of D0. In addition, the incorporation of BT unit encourages the π spacer-cyanoacrylic acid group to adopt a more planar structure to enhance the internal charge transfer process. Similar features for D0 and D2 are also found. Compared with benzene ring, the pyridine unit is π -electron deficient. If the benzene in the BT unit is replaced with a pyridine group, the new unit, thiadiazolo[3,4-c]pyridine (PyT), is expected to be one stronger electron-deficient unit, and our simulations confirm this conjecture. Comparing D1 and D2, D3 and D4, replacing the electron-deficient BT unit with the more electron-deficient PyT units effectively lowers the LUMO energy of ca 0.15 eV and therefore decreases the band gap.

The thiophene unit is electron-rich, and it has been demonstrated that incorporating thiophene units into the polymer backbone can decrease the band gap by increasing HOMO energy level [29]. One can also decrease the electron-richness of the thiophene unit by fusing

it with a less electron-rich benzene unit, and NDT monomer with a naphthalene core incorporated to decrease the electron-richness of the flanked bithiophene unit is such a case. Comparing D1 and D3, the incorporation of NDT unit into the π -linkage (meanwhile connection to the donor TPA) raises the HOMO energy level of D3 to -4.98 eV compared with that of D1 (-5.19 eV). Because the other common unit, BT, dictates similar LUMO energy levels, the HOMO-LUMO gap of D3 is 0.3 eV smaller than that of D1, as shown in **Figure 3**. Similar features of energy level positions between D2 and D4 are also shown. Therefore, we can tune the HOMO and LUMO energy levels by structural modifications of the TPA dyes via incorporating different units as the π -spacers. From D0 to D4, the HOMO-LUMO gap significantly decreases from 2.44 eV for D0 to 1.70 eV for D4. We should notice that B3LYP/6-31G(d,p) level calculations tend to over-estimated the HOMO and LUMO energies for some TPA-based dyes, compared to experimental data [44]. But the relative energy level position and the HOMO-LUMO gap of some structurally similar TPA dyes are reasonable and agree with the experimental trend [12].

For all dyes considered here, the simulated LUMOs of TPA derivatives dyes all lie above the TiO₂ conduction band edge (–4.00 eV vs. vacuum [1]), all providing favorable thermodynamic driving force for electron injection from the dye's excited state to the TiO₂ conduction band edge. The electron collection yields and the dye regeneration yields depend on the potential difference between the oxidized dyes and the redox couple. For the sensitizers with similar structures for which the HOMO levels are much positive than the redox potential, sufficient driving forces will lead to longer effective electron-diffusion lengths and efficient dye regenerations almost remains [45]. Our simulations demonstrated that the HOMO of all dyes lies below the iodide redox potential (–4.60 eV vs. vacuum [17]), leading to fast dye regeneration and avoiding the charge recombination between oxidized dye molecules and photo-injected electrons in the nanocrystalline TiO₂ film.

3.3 Excitations

For a reasonable computational effort, the state of the art DFT/TDDFT computational methodologies provide resonable results and reproduce well the optical properties of various Ru(II) complexes [46,47] and metal-free organic dyes [34,48-50]. We first examined the effect of the functionals on the excitation energies of the lowest excited state λ_{max} . Table 1 presents a comparison between simulated λ_{max} using different functionals and experimental maxima for D1. Experimentally, Lin and co-workers have synthesized D1 dye (namely S1 in their work) with a benzothiadiazole unit into the conjugated backbone, and the D1 dye showed absorption maxima at 491 nm in THF [25]. We found from **Table 1** that the choice of functionals reveals great effect on the excitation energy. PW91, a pure DFT functional that

depends only on the local one-electron density and its gradient, cannot describe the excitation properties of D1 correctly, since it presents the largest underestimate of the excitation energy of 1.3 eV to the experimental data. The B3LYP functional also underestimates the lowest excitation energy with a large error of 0.8 eV to the experimental data. Compared with B3LYP (20% HF), PBE0 and BHandH, which benefits from the more amount of exact exchange (25% HF for PBE0 and 50% HF for BHandH), give a relatively better performance in the prediction of lowest-lying excitations. Especially for BHandH, the discrepancy between calculated and experimental results is within 20 nm. The CAM-B3LYP functional has been reported to provide reliable results for some organic dyes, with excitation energies very close to experimental data when the bulk solvation effects are included [50]. Our simulated results show that the CAM-B3LYP functional, combined with the 6-311+G(d,p) basis set, gives the excitation energies of the lowest excited state at 501 nm in THF solvent with a oscillator strength of 1.44, presenting most reliable UV/Vis prediction of D1 dye absorption spectra. Indeed, our simulations provide excitation energies for the lowest excited state with a mean absolute deviation of 10 nm, which is the generally accepted upper limit required for the design of new industrial dyes. Therefore, on the basis of the agreement with experimental data, CAM-B3LYP is the functional of choice for the UV/Vis spectra calculation.

Table 1 Experimental absorption maxima and computed excitation energies of the lowest excited state λ max (nm) for the dye D1 in tetrahydrofuran solution, together with the calculated oscillator strength f and excitation configuration.

	λ_{max}	f	Main configuration
PW91	994	0.6079	H→L 0.70 (98%)
B3LYP	707	0.8020	H→L 0.70 (98%)
PBE0	653	0.8957	H→L 0.70 (98%)
BHandH	511	1.4121	H→L 0.63 (78%)
CAM-B3LYP	501	1.4381	H→L 0.59 (70%)
Experiments [25]	491		

The simulated electronic absorption spectra of D0-D4 dissolved in dichloromethane solvent at CPCM-TDCAM-B3LYP/6-311+G(d,p) level of theory are shown in **Figure 4**, and **Table 2** lists the excitation energies of the lowest excited state. Our simulations have demonstrated two allowed excited states in the UV/Vis region characterized by large transition probabilities: an first sharp peak in the 400–600 nm region and a second absorption main band with high intensity near the 300 nm region, which is consistent with

experimental and theoretical investigations [12, 34, 44]. Compared with dye D0 with phenylene as the π -spacer, the introduction of BT, PyT, NDT-BT, and NDT-PyT moieties reveals strong the effects on the UV/Vis spectra and leads to remarkably red-shifted adsorption bands. In case of D1, the incorporation of a BT unit displays a remarkable 85 nm red-shifted absorption than D0. As has been demonstrated in Section 3.2, the BT unit is a low-band gap chromophore which can significantly affect the electronic structure of the dye and reduces the band gap tremendously by lowering the LUMO energy level and therefore resulting to a red-shifted adsorption [24]. PyT is expected be one stronger electron-deficient unit than BT. **Figure 4** demonstrates that D2 showed more red-shifted absorption of 118 nm than D0, which might enhance the light harvesting of the sensitizers. For the D1 and D2 with similar structural architecture, D2 display 33 nm red-shifted absorption band when compared to the D1, due to the fact that the pyridine unit is a more stronger π -electron deficient unit.

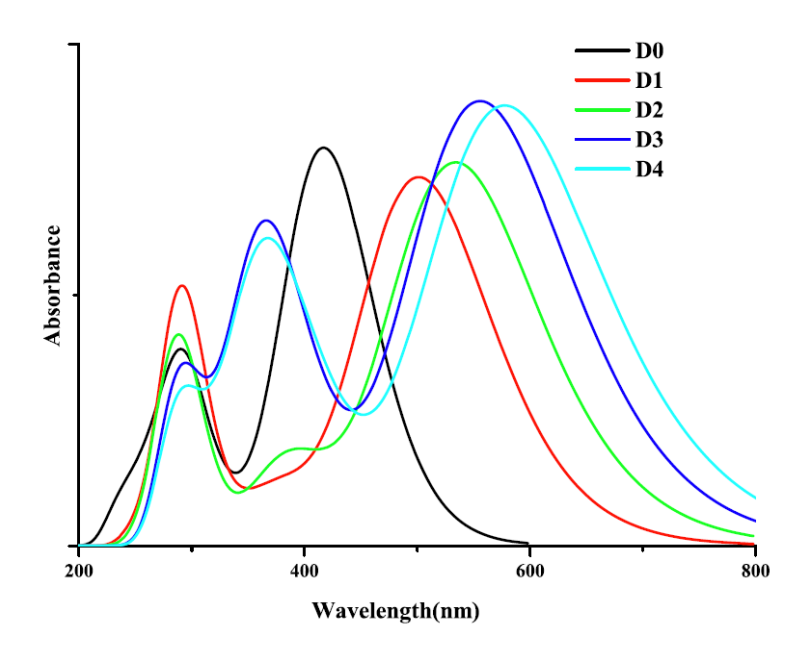


Figure 4: The calculated absorption spectra for the TPA dyes dissolved in dichloromethane at CPCM-TDCAM-B3LYP/6-311+G(d,p)//B3LYP/6-31G(d,p) level of theory.

Previous experiments have demonstrated that the optical absorption of the organic dyes is red-shifted on extension of the π conjugation by the incorporation of electron-deficient segments [22, 24]. You and coworkers have synthesized a series of narrow band gap polymers incorporating NDT units for organic solar cells [29-32]. For example, recently they constructed a library of polymers employing the NDT and BT units as the weak donor and

the strong acceptor, respectively. The PNDT-BT is shown to have both a low HOMO energy level of -5.35 eV and a narrow band gap of 1.59 eV, and a noticeably high $V_{\rm oc}$ of 0.83 V was received from the BHJ device of PNDT-BT blended with PCBM [29]. Inspired by You's work, dyes D3 and D4 are constructed with the presence of NDT group to the π spacer. **Figure 4** clearly shows that the incorporation of NDT and electron-deficient thiadiazole derivatives into the spacer shifts the absorption band to the red portion of the solar spectrum. Organic dye D3 exhibits absorbance maxima at 556 nm, which red-shifts 139 nm relative to D0 dye. While for D4, on introducing NDT and more electron-deficient PyT unit, the higher wavelength band grows in intensity with a significant red-shift of 161 nm, compared to D0 dye. It is known that a broad absorption band covering the whole visible and some of the near-infrared region is favorable to attain good overlap with the solar spectrum to produce an enhanced photocurrent response. The newly designed dyes D2-D4 gradually red-shift the adsorption peak from 535 to 578 nm, which is favorable for a larger photoresponse in red portion of solar spectrum, compared to the D0 dye.

Table 2 The calculated dipole-allowed lowest excited state λ_{max} (nm) for the dyes D0-D4 in CH₂Cl₂ solution provided by CPCM-TDCAM-B3LYP/6-311+G(d,p). The calculated oscillator strength f and main excitation configuration are also listed.

Dyes	λ_{max}	f	Main configuration
D0	417	1.5615	$H \to L$ 0.48 (46%)
	417		$H-1 \rightarrow L 0.48 \ (46\%)$
D1	502	1.4453	$H \to L$ 0.59 (70%)
	302		$H-1 \rightarrow L 0.34 (23\%)$
D2	535	1.5048	$H \rightarrow L$ 0.63 (79%)
D3	EE(1.7460	$H \to L$ 0.53 (56%)
	556		$H-1 \rightarrow L 0.38 (29\%)$
D4	E70	1.7279	$H \to L$ 0.54 (58%)
	578		$H-1 \rightarrow L 0.40 (32\%)$

The light harvesting efficiency (LHE) of the dye sensitizer should be as high as possible to maximize the photocurrent response. LHE can be quantified by eqn (2), if there is just one absorption for electron injection [51]

$$LHE = 1 - 10^{-A} = 1 - 10^{-f}$$
 (2)

where A(f) is the absorption (oscillator strength) of the dye associated to the λ_{max} . Here the LHE parameter relates to the light harvesting ability of the dye sensitizer corresponding to

the intramolecular charge transfer transition.

We also found that the calculated oscillator strength for D3 and D4 is larger than that of D0. The increased oscillator strength might enhance the LHE value and give rise to the increasing overlap with the solar spectrum, especially at the visible range. The increase of LHE factor is related to the increasing coplanarity between the spacer units and the TPA phenyl group, which might be encouraged by the strong internal charge transfer interaction between NDT and BT units [29]. For organic dyes, the nonplanar conformations tend to hamper the electronic conjugation between the donor and the acceptor groups, resulting in a decreased intrmolecular charge transfer oscillator strength [52]. We conclude that compared with D0, dyes D1-D4 with electron-deficient units demonstrate obvious improvements in optical properties, which is hypothesized to benefit the light harvesting properties of the dyes when used in the DSSCs.

3.4 Dye/TiO2 interacting system

For a better understanding of the electronic structure and the electron transfer features during the light excitation and the electronic coupling between excited-state dye and the TiO₂ conduction band, we also optimized the geometry of dye/ TiO₂ interface and studied the energy levels for the interacting and non-interacting species of dyes D0-D4 and (TiO2)46 nanocluster. The structure and the electronic excited states of the interface determine the efficiency of the electron injection from the excited state dye into the conduction band of the semiconductor. The theoretical simulation of the dye/TiO2 interface is an important step towards the optimization of DSSCs. We have performed a combination of DFT, DFTB, and TDDFT calculations on the structural and electronic features of the interacting system of some TPA organic dyes on TiO2 interface, and reasonable results which are consistent with experimental data were received [44,53]. Using the same theoretical approach, here we studied the D0-D4/(TiO₂)₄₆ complexes. The optimized geometry of bidentate adsorption mode for D3/(TiO₂)₄₆ is shown in **Figure 5**. We found that after adsorption to the (TiO₂)₄₆ nanocluster, the dye sensitizer almost remains its structure, except for the anchoring group. The formation of two additional Ti-O bonds, together with the binding of one hydrogen atom to the TiO2 surface oxygen atom, leads to considerable rearrangements of the (TiO2)46 nanocluster. The interactions between the dyes and the TiO2 surface are rather strong, with average calculated distances between the carboxylic oxygen atoms and the TiO2 surface (O-Ti bond) of 2.0-2.1 Å. For all the dyes considered, the structures of dye/(TiO₂)₄₆ show similar features as D3/(TiO₂)₄₆. The results for the energy levels of D3/(TiO₂)₄₆ interacting system are represented in Figure 6. The selective isosurfaces of the D3 and D3/TiO2 system were also drawn, including the HOMO, LUMO and the interacting orbitals, as shown in the

insets. From **Figure 6** we found that the features of energy diagram of the non-interacting and interacting dye D3 and the $(TiO_2)_{46}$ modes are similar to those of dye C217 and $(TiO_2)_{46}$ cluster [44]. For the interacting system, the HOMO solely locates on the dye part, while the LUMO is just localized on the TiO_2 conduction band. The dye LUMO energy level has no coupling to the TiO_2 conduction band and will decrease due to the interaction with TiO_2 . The interacting LUMO orbitals that have non-negligible contributions from the free dye LUMO are situated higher up in the conduction band (LUMO+14) for D3/ TiO_2 , as demonstrated in the insets. The interacting orbital shows strong mixing of adsorbate π^* and TiO_2 3d orbitals. It is well known that during light exitation, the electronic coupling and electron transfer take place between dye's LUMO and the TiO_2 conduction band. The spatial orientation of the molecular orbitals for the isolated sensitizer and the TiO_2 definite from the TPA through the TiO_3 bridge to the surface-bound cyanoacrylate, thus facilitating strong coupling of the excited state wave function with the $TiTO_3$ matrix.

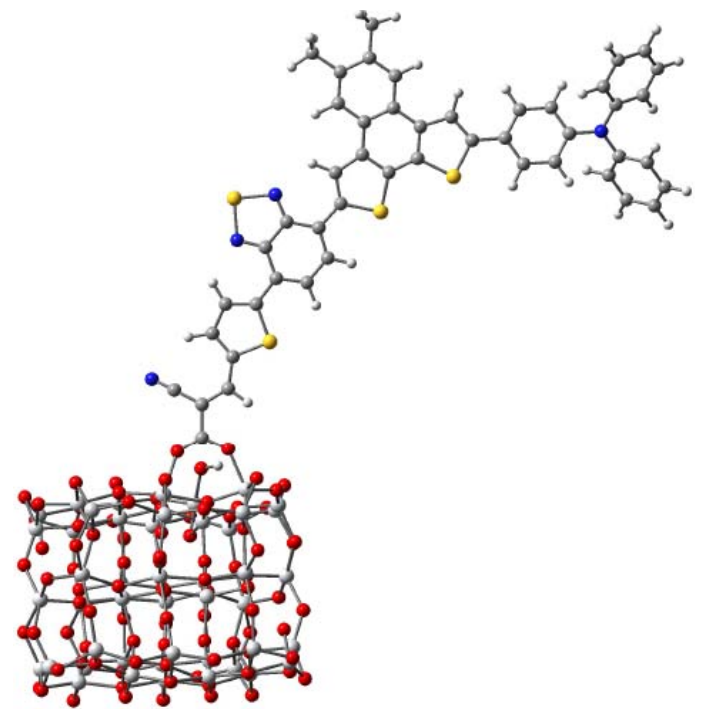


Figure 5: Optimized geometry of a bidentate binding mode of the D3 dye on the (TiO₂)₄₆ nanoparticle.

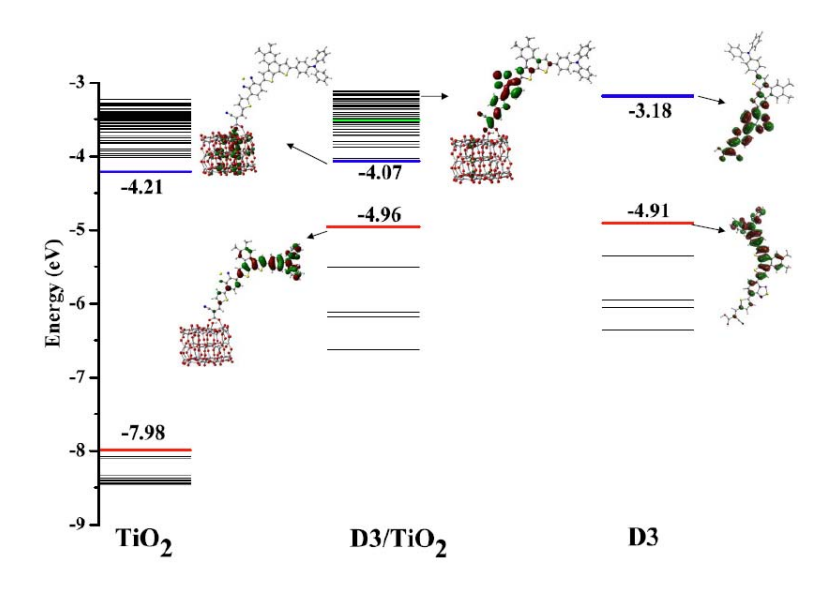


Figure 6: Schematic energy diagram of the non-interacting and interacting sensitizer D3 and the (TiO₂)₄₆ nanoparticle. Energy in eV. The insets are the isosurfaces of the HOMO, LUMO and the interacting orbital of the dye and dye/TiO₂ systems, respectively.

Although the features of energy diagram of all the dyes studied are similar, we found that the interacting orbitals are located at energy-lower positions when electron-deficient groups are introduced. The interaction orbital energies and positions of dye/TiO₂ system are -3.10 eV (LUMO+40), -3.48 eV (LUMO+14), -3.65 eV (LUMO+9), -3.51 (LUMO+14) and -3.66 eV (LUMO+9) for D0-D4, respectively, which are consistent with the free dye's LUMO positions. It is well known that during the light excitation, the electronic coupling and electron transfer occur between dye's LUMO and the TiO₂ conduction band. Thus the positions of the LUMO levels determined the interaction orbital position between the dye and TiO₂ conduction band. As can be found from **Figure 3**, after incorporation of electron deficient units, the LUMO levels of the dyes decreased evidently. The introduction of electron-deficient groups in the π spacer results in deceasing interaction orbital energies. Therefore, the π spacer and the incorporation of electron-deficient units of similar TPA dyes show evident effects on the electronic properties for the dye/TiO₂ complexes.

4 Conclusions

We designed a series of triphenylamine (TPA)-based sensitizers incorporating electron-deficient thiadiazole derivatives as the π -spacer for dye-sensitized solar cells

(DSSCs). High level calculations based on density functional tight-binding (DFTB), density functional theory (DFT), and time-dependent DFT (TDDFT) are performed. Our simulations show that the electron-deficient thiadiazole derivatives demonstrated great effect on the spectra and electrochemical properties of the TPA-based organic dyes. Compared with the model compound which adopts a phenylene unit as the π -spacer, the newly designed dyes display significantly enhanced spectral responses in the UV/Vis solar spectrum, due to the significantly much deeper LUMO levels. The dyes/(TiO₂)₄₆ anatase nanoparticle systems were also simulated to show the electronic structures at the interface, and we show that when binding to a (TiO₂)₄₆ nanoparticle, strong electronic coupling between dye's LUMO and the TiO₂ conduction band is found, which is favorable for an efficient electron injection from the dye onto the semiconductor surface. Our simulations show that the newly constructed dyes D2, D3, and D4 demonstrate desirable energetic and spectroscopic parameters, and they are expected to be efficient sensitizers for DSSCs.

Acknowledgments

This work was supported by the National Natural Science Foundation of China (grant no. 21103169) and the "100-Talent Program" of the Chinese Academy of Sciences.

References

- [1] M. Grätzel, Photoelectrochemical cells, Nature 414 (2001), 338-344.
- [3] B. Oregan, M. Grätzel, A low cost, high-efficiency solar-cell based on dye-sensitized colloidal TiO₂ film, Nature 353 (1991), 737-740.
- [2] M. Grätzel, Dye-sensitized solar cells, J. Photochem. Photobiol. C-Photochem. Rev. 4 (2003), 145-153.
- [4] M. Grätzel, Recent advances in sensitized mesoscopic solar cells, Accounts Chem. Res. 42 (2009), 1788-1798
- [5] M.K. Nazeeruddin, F. De Angelis, S. Fantacci, A. Selloni, G. Viscardi, P. Liska, S. Ito, T. Bessho, M. Gratzel, Combined experimental and DFT-TDDFT computational study of photoelectrochemical cell ruthenium sensitizers, J. Am. Chem. Soc. 127 (2005), 16835-16847.
- [6] M. Gratzel, Conversion of sunlight to electric power by nanocrystalline dye-sensitized solar cells, J. Photoch. Photobio. A 164 (2004), 3-14.
- [7] A. Mishra, M.K.R. Fischer, P. Bauerle, Metal-free organic dyes for dye-sensitized solar cells: from structure: property relationships to design rules, Angew. Chem. Int. Ed. 48 (2009), 2474-2499.
- [8] Z.S. Wang, Y. Cui, K. Hara, Y. Dan-Oh, C. Kasada, A. Shinpo, A high-light-harvesting-efficiency coumarin dye for stable dye-sensitized solar cells, Adv. Mater. 19 (2007), 1138-1141.

- [9] T. Horiuchi, H. Miura, K. Sumioka, S. Uchida, High efficiency of dye-sensitized solar cells based on metal-free indoline dyes, J. Am. Chem. Soc. 126 (2004), 12218-12219.
- [10] S. Kim, G.K. Mor, M. Paulose, O.K. Varghese, C. Baik, C.A. Grimes, Molecular design of near-IR harvesting unsymmetrical squaraine dyes, Langmuir 26 (2010), 13486-13492.
- [11] C. Li, J.H. Yum, S.J. Moon, A. Herrmann, F. Eickemeyer, N.G. Pschirer, P. Erk, J. Schoeboom, K. Mullen, M. Grätzel, M.K. Nazeeruddin, An improved perylene sensitizer for solar cell applications, ChemSusChem. 1 (2008), 615-618.
- [12] G.L. Zhang, H. Bala, Y.M. Cheng, D. Shi, X.J. Lv, Q.J. Yu, P. Wang, High efficiency and stable dye-sensitized solar cells with an organic chromophore featuring a binary π -conjugated spacer, Chem. Commun. (2009), 2198-2200.
- [13] D.P. Hagberg, J.H. Yum, H. Lee, F.De Angelis, T. Marinado, K.M. Karlsson, R. Humphry-Baker, L.C. Sun, A. Hagfeldt, M. Grätzel, M.K. Nazeeruddin, Molecular engineering of organic sensitizers for dye-sensitized solar cell applications, J. Am. Chem. Soc. 130 (2008), 6259-6266.
- [14] R.Z. Li, J.Y. Liu, N. Cai, M. Zhang, P. Wang, Synchronously reduced surface states, charge recombination, and light absorption length for high-performance organic dye-sensitized solar cells, J. Phys. Chem. B 114 (2010), 4461–4464.
- [15] W.D. Zeng, Y.M. Cao, Y. Bai, Y.H. Wang, Y.S. Shi, M. Zhang, F.F. Wang, C.Y. Pan, P. Wang, Efficient dye-sensitized solar cells with an organic photosensitizer featuring orderly conjugated ethylenedioxythiophene and dithienosilole blocks, Chem. Mater. 22 (2010), 1915-1925.
- [16] H.N Tian, X.C. Yang, R.K. Chen, R. Zhang, A. Hagfeldt, L.C Sun, Effect of different dye baths and dye-structures on the performance of dye-sensitized solar cells based on triphenylamine dyes, J. Phys. Chem. C 112 (2008), 11023-11033.
- [17] G.L. Zhang, Y. Bai, R.Z. Li, D. Shi, S. Wenger, S.M. Zakeeruddin, M. Grätzel, P. Wang, Employ a bisthienothiophene linker to construct an organic chromophore for efficient and stable dye-sensitized solar cells, Energ. Environ. Sci. 2 (2009), 92-95.
- [18] H. Choi, D. Kim, F. Teocoli, C. Kim, K. Song, J.H. Yum, J. Ko, M.K. Nazeeruddin, M. Grätzel, High molar extinction coefficient organic sensitizers for efficient dye-sensitized solar cells, Chem.-Eur. J. 16 (2010), 1193-1201.
- [19] H. Choi, H. Choi, S. Paek, K. Song, M.-S. Kang, J. Ko, Novel organic sensitizers with a quinoline unit for efficient dye-sensitized solar cells, Bull. Korean Chem. Soc. 31 (2010), 125-132.
- [20] Y.-T. Li, C.-L. Chen, Y.-Y. Hsu, H.-C. Hsu, Y. Chi, B.-S. Chen, W.-H. Liu, C.-H. Lai, T.-Y. Lin, P.-T. Chou, Donor-acceptor organic sensitizers assembled with isoxazole or its derivative 3-oxopropanenitrile, Tetrahedron 66 (2010), 4223-4229.
- [21] C.-H. Chen, Y.-C. Hsu, H.-H. Chou, K. R. J. Thomas, J. T. Lin, C.-P. Hsu, Dipolar compounds containing fluorene and heteroaromatic ring as conjugating bridge for high-performance dye-sensitized solar cells, Chem.-Eur. J. 16 (2010), 3184-3193.

- [22] L.Y. Lin, C.H. Tsai, K.T. Wong, T.W. Huang, C.C. Wu, S.H. Chou, F. Lin, S.H. Chen, A.I. Tsai, Efficient organic DSSC sensitizers bearing an electron-deficient pyrimidine as an effective p-spacer, J. Mater. Chem. 21 (2011), 5950-5958.
- [23] D.H. Lee, M.J. Lee, H.M. Song, B.J. Song, K.D. Seo, M. Pastore, C. Anselmi, S. Fantacci, F.De Angelis, M.K. Nazeeruddin, M. Grätzel, H.K. Kim, Organic dyes incorporating low-band-gap chromophores based on p-extended benzothiadiazole for dye-sensitized solar cells, Dyes and Pigments 91 (2011), 192-198.
- [24] K.R.J. Thomas, A. Baheti, Y.-C. Hsu, K.-C. Ho, J.T. Lin, Electro-optical properties of new anthracene based organic dyes for dye-sensitized solar cells, Dyes and Pigments 91 (2011), 33-43.
- [25] M. Velusamy, K.R.J. Thomas, J.T. Lin, Y.C. Hsu, K.C. Ho, Organic dyes incorporating lowband-gap chromophores for dye-sensitized solar cells, Org Lett 7 (2005), 1899-1902.
- [26] M.F. Xu, R.Z. Li, N. Pootrakulchote, D. Shi, J. Guo, Z.H. Yi, S.M. Zakeeruddin, M. Grätzel, P. Wang, Energy-level and molecular engineering of organic D-pi-A sensitizers in dye-sensitized solar cells, J. Phys. Chem. C 112 (2008), 19770-19776.
- [27] J.T. Lin, P.-C. Chen, Y.-S. Yen, Y.-C. Hsu, H.-H. Chou, M.-C. P. Yeh, Organic dyes containing furan moiety for high-performance dye-sensitized solar cells, Org. Lett. 11 (2009), 97-100.
- [28] Y.-S. Yen, Y.-C. Hsu, J.T. Lin, C.-W. Chang, C.-P. Hsu, D.-J. Yin, Pyrrole-based organic dyes for dye-sensitized solar cells, J. Phys. Chem. C 112 (2008), 12557-12567.
- [29] H. Zhou, L. Yang, S. Stoneking, W. You, A weak donor-strong acceptor strategy to design ideal polymers for organic solar cells, ACS Appl. Mater. Interfaces 2 (2010), 1377-1383.
- [30] H. Zhou, L. Yang, S.C. Price, K.J. Knight, W. You, Enhanced photovoltaic performance of low-bandgap polymers with deep LUMO Levels, Angew. Chem. Int. Ed. 49 (2010), 7992-7995.
- [31] H. Zhou, L. Yang, S. Liu, W. You, A tale of current and voltage interplay of band gap and energy levels of conjugated polymers in bulk heterojunctionsolar cells, Macromolecules 43 (2010), 10390-10396.
- [32] S.A. Miller, A.C. Stuart, J.M. Womick, H. Zhou, W. You, A.M. Moran, Excited-state photophysics in a low band gap polymer with high photovoltaic efficiency, J. Phys. Chem. C 115 (2011), 2371-2380.
- [33] M. Elstner, D. Porezag, G. Jungnickel, J. Elsner, M. Haugk, T. Frauenheim, S. Suhai, G. Seifert, Self-consistent-charge density-functional tight-binding method for simulations of complex materials properties, Phys. Rev. B 58 (1998), 7260-7268.
- [34] J. Preat, C. Michaux, D. Jacquemin, E.A. Perpete, Enhanced efficiency of organic dye-sensitized solar cells: triphenylamine derivatives, J. Phys. Chem. C 113 (2009), 16821-16833.
- [35] J.P. Perdew, K. Burke, Y. Wang, Generalized gradient approximation for the exchange-correlation hole of a many-electron system, Phys. Rev. B, 54 (1996), 16533.
- [36] A.D. Becke, A new mixing of Hartree-Fock and local density-functional theories J. Chem. Phys. 98 (1993), 1372-1377

- [37] C. Adamo, V. Barone, Toward reliable density functional methods without adjustable parameters: The PBE0 model, J. Chem. Phys. 110 (1999), 6158-6170.
- [38] A.D. Becke, Density-functional thermochemistry. III. The role of exact exchange, J. Chem. Phys., 98 (1993), 5648-5652.
- [39] T. Yanai, D.P. Tew, N.C. Handy, A new hybrid exchange-correlation functional using the Coulomb-attenuating method (CAM-B3LYP), Chem. Phys. Lett. 393 (2004), 51-57.
- [40] M. Cossi, V. Barone, Time-dependent density functional theory for molecules in liquid solutions, J. Chem. Phys. 115 (2001), 4708-4717.
- [41] M.J. Frisch, G.W. Trucks, H.B. Schlegel, G.E. Scuseria, M.A. Robb, J.R. Cheeseman, J.A. Montgomery, T. Vreven, K.N. Kudin, J.C. Burant, J.M. Millam, S.S. Iyengar, J. Tomasi, V. Barone, B. Mennucci, M. Cossi, G. Scalmani, N. Rega, G.A. Petersson, H. Nakatsuji, M. Hada, M. Ehara, K. Toyota, R. Fukuda, J. Hasegawa, M. Ishida, T. Nakajima, Y. Honda, O. Kitao, H. Nakai, M. Klene, X. Li, J.E. Knox, H.P. Hratchian, J.B. Cross, V. Bakken, C. Adamo, J. Jaramillo, R. Gomperts, R.E. Stratmann, O. Yazyev, A.J. Austin, R. Cammi, C. Pomelli, J.W. Ochterski, P.Y. Ayala, K. Morokuma, G.A. Voth, P. Salvador, J.J. Dannenberg, V.G. Zakrzewski, S. Dapprich, A.D. Daniels, M.C. Strain, O. Farkas, D.K. Malick, A.D. Rabuck, K. Raghavachari, J.B. Foresman, J.V. Ortiz, Q. Cui, A.G. Baboul, S. Clifford, J. Cioslowski, B.B. Stefanov, G. Liu, A. Liashenko, P. Piskorz, I. Komaromi, R.L. Martin, D.J. Fox, T. Keith, A.M.A. Laham, C.Y. Peng, A. Nanayakkara, M. Challacombe, P.M.W. Gill, B. Johnson, W. Chen, M.W. Wong, C. Gonzalez, J.A. Pople, Gaussian 09, Revision A02, Gaussian Inc, Wallingford CT, 2009.
- [42] B. Aradi, B. Hourahine, T. Frauenheim, DFTB+, a sparse matrix-based implementation of the DFTB method, J. Phys. Chem. A 111 (2007), 5678-5684.
- [43] P. Qin, X.C. Yang, R.K. Chen, L.C. Sun, T. Marinado, T. Edvinsson, G. Boschloo, A. Hagfeldt, Influence of pi-conjugation units in organic dyes for dye-sensitized solar cells, J. Phys. Chem. C 111 (2007), 1853-1860.
- [44] W.J Fan, D.Z Tan, W.Q. Deng, Theoretical investigation of triphenylamine dye/titanium dioxide interface for dye-sensitized solar cells, Phys. Chem. Chem. Phys. 13 (2011), 16159-16167.
- [45] C. Teng, X.C. Yang, S.F. Li, M. Cheng, A. Hagfeldt, L.Z. Wu, L.C. Sun, Tuning the HOMO energy levels of organic dyes for dye-sensitized solar cells based on Br/Br₃- electrolytes, Chem. Eur. J. 16 (2010), 13127-13138.
- [46] L. Salassa, C. Garino, G. Salassa, R. Gobetto, C. Nervi, Mechanism of ligand photodissociation in photoactivable Ru(bpy)(2)L-2 (2+) complexes: A density functional theory study, J. Am. Chem. Soc. 130 (2008), 9590-9597.
- [47] M.K. Nazeeruddin, Q. Wang, L. Cevey, V. Aranyos, P. Liska, E. Figgemeier, C. Klein, N. Hirata, S. Koops, S.A. Haque, J.R. Durrant, A. Hagfeldt, A.B.P. Lever, M. Gratzel, DFT-INDO/S modeling of new high molar extinction coefficient charge-transfer sensitizers for solar cell applications, Inorg. Chem. 45 (2006), 787-797.

- [48] S. Kim, J.K. Lee, S.O. Kang, J. Ko, J.H. Yum, S. Fantacci, F. De Angelis, D. Di Censo, M.K. Nazeeruddin, M. Gratzel, Molecular engineering of organic sensitizers for solar cell applications, J. Am. Chem. Soc. 128 (2006), 16701-16707.
- [49] D. Jacquemin, V. Wathelet, E.A. Perpete, C. Adamo, Extensive TD-DFT Benchmark: Singlet-Excited States of Organic Molecules, J. Chem. Theory Comput. 5 (2009), 2420-2435.
- [50] M. Pastore, E. Mosconi, F.De Angelis, M. Grätzel, A computational investigation of organic dyes for dye-sensitized solar cells: benchmark, strategies, and open issues, J. Phys. Chem. C 114 (2010), 7205-7212.
- [51] J. Preat, A. Hagfeldt, E.A. Perpète, Investigation of the photoinduced electron injection processes for p-type triphenylamine-sensitized solar cells, Energy Environ. Sci. 4 (2011), 4537-4549.
- [52] D. Jacquemin, J. Preat, V. Wathelet, J.M. André, E.A. Perpéte, Substitution effects on the visible spectra of 1,4-diNHPh-9,10-anthraquinones, Chem. Phys. Lett. 405 (2005), 429-433.
- [53] W.J. Fan, D.Z. Tan, W.Q. Deng, Acene-modified triphenylamine dyes for dye-sensitized solar cells: a computational study, Chemphyschem. 13 (2012), 2051-2060.